

Responses of recurrent nets of asymmetric ON and OFF cells

J r mie Lefebvre · Andr  Longtin · Victor G. LeBlanc

Received: 7 June 2010 / Accepted: 17 October 2010 /
Published online: 20 November 2010
  Springer Science+Business Media B.V. 2010

Abstract A neural field model of ON and OFF cells with all-to-all inhibitory feedback is investigated. External spatiotemporal stimuli drive the ON and OFF cells with, respectively, direct and inverted polarity. The dynamic differences between networks built of ON and OFF cells (“ON/OFF”) and those having only ON cells (“ON/ON”) are described for the general case where ON and OFF cells can have different spontaneous firing rates; this asymmetric case is generic. Neural responses to nonhomogeneous static and time-periodic inputs are analyzed in regimes close to and away from self-oscillation. Static stimuli can cause oscillatory behavior for certain asymmetry levels. Time-periodic stimuli expose dynamical differences between ON/OFF and ON/ON nets. Outside the stimulated region, we show that ON/OFF nets exhibit frequency doubling, while ON/ON nets cannot. On the other hand, ON/ON networks show antiphase responses between stimulated and unstimulated regions, an effect that does not rely on specific receptive field circuitry. An analysis of the resonance properties of both net types reveals that ON/OFF nets exhibit larger response amplitude. Numerical simulations of the neural field models agree with theoretical predictions for localized static and time-periodic forcing. This is also the case for simulations of a network of noisy integrate-and-fire neurons. We finally discuss the application of the model to the electrosensory system and to frequency-doubling effects in retina.

Keywords Recurrent connections · Delayed feedback · Bifurcations · ON and OFF cells

J. Lefebvre (✉) · A. Longtin
Department of Physics, University of Ottawa, 50 Louis Pasteur, Ottawa, ON, K1N-6N5, Canada
e-mail: jlefe@uottawa.ca, champvectoriel@hotmail.com

V. G. LeBlanc
Department of Mathematics and Statistics, University of Ottawa, 585 King Edward Avenue, Ottawa,
ON, K1N 6N5, Canada

1 Introduction

Information processing along sensory pathways relies both on single cell properties and network geometry. A dominant feature of these pathways is feedback between successive anatomically distinct neural populations or nuclei, as well as connections within each nucleus. At some point along a sensory pathway, feedback appears and shapes the integration and processing of spatiotemporal inputs in ways that are yet to be fully understood. Much experimental and theoretical research is in fact devoted to this issue. In particular, feedback may underlie the appearance of oscillatory activity when the input has certain attributes. Such oscillations, which have been linked to information processing tasks in many areas of the nervous system, often emerge via inhibitory feedback connections [1–5] and especially when delays are present [3, 6, 7]. Large delays can even produce multistability [3, 8].

Localized inputs are known to cause localized increases in activity or “bumps” that can be maintained as long as the input is on. Oscillatory responses to static input can also occur because the spatial profile of the input induces an Andronov–Hopf bifurcation in the recurrent network [9, 10]. In other cases, the degree of spatial correlation in an otherwise stochastic input determines the onset of oscillation [6, 11]. Such oscillations, however, are not always triggered by a static stimulus. Time-periodic inputs also recruit the temporal integration properties of the sensory pathway and drive recurrent connections. Investigations of these issues have also moved on to more realistic two-population systems [12, 13], where all cells respond the same way to external input.

In fact, the bulk of the research on driven neural networks considers that all cells respond in the same manner to the external stimulus. However, most sensory systems are made up, at some point along the way, of two subpopulations, namely ON and OFF cells [14–17]. This is true for the visual, auditory, pain, and electrosensory systems. The ON and OFF populations are distinguished by their response to inputs. ON cells receive input directly and increase their firing activity when the input increases. In contrast, OFF cells receive an inverted image of incoming stimuli, transmitted via inhibitory interneurons [14]. Secondly, ON and OFF cells will generally fire at different mean rates even in the absence of an external input stimulus. Examples of such asymmetrical zero-input activity between ON and OFF populations have been observed in the electrosensory system [18] and the visual system [19], where the distribution of firing rates for ON cells has a different mean than that for OFF cells.

The distinct responses of ON and OFF populations with different intrinsic spontaneous rates is the focus of our paper. We characterize this rate difference as an “asymmetry”. This situation is usually described as one wherein the two populations have distinct firing rates, where “spontaneous” refers to the fact that there is no external stimulation. But this is to be distinguished from another common use of the term “spontaneous” where the context is one in which the cell is isolated from both the external stimulus and the feedback. The firing of the cells at different mean rates is usually attributed to the fact that there is either local circuitry that delivers different net currents into the cells or that the intrinsic physiological characteristics such as leak conductance are different, or both. It is already an interesting question to infer these “intrinsic spontaneous” rates from the spontaneous rates measured when the feedback is intact (with zero input in both cases). In some settings, it is possible to pharmacologically or surgically impair the feedback to reveal the intrinsic spontaneous rates.

In this article, we propose a comprehensive comparative study of input response dynamics of networks built of ON and Off cell populations (ON/OFF nets) compared

to those of networks built solely of excitatory cells (ON/ON nets). In [20], a variety of stimulus responses in an ON/OFF net have been presented in the context of a neural field model, with much additional support from simulations of networks of noisy leaky integrate-and-fire (LIF) neurons. The parameters that influenced the number of steady states of the network dynamics and their stability were analyzed. In particular, it was shown that unequal spontaneous firing rates or “asymmetry” can strongly influence the number of steady states and their stability, but without demonstrating stronger implications of this asymmetry as we do here. Further, the response features discussed in [20] gave little information about the sensory processing differences and benefits enabled by the combined action of multiple neural populations. It is especially important to determine whether a recurrent symmetric ON/OFF net, which our previous study showed is less likely to exhibit self-sustained oscillations in response to a static input, is still less likely to do so when the symmetry condition is relaxed. Our results below show that, surprisingly, this is not the case, i.e., asymmetric ON/OFF nets can be more prone to oscillate.

To address the fundamental questions of the advantages versus disadvantages of an ON/OFF organization, a systematic comparison of stimulus-induced states in networks with and without OFF cells is essential. This will enable us to distinguish response features due to feedback nonlinearities from those caused solely by the characteristic inhibitory responses of OFF cells to input. Our paper builds on the recent results on recurrent networks of ON and OFF cells in [20] and can be seen as the natural extension of that work. It first extends its predictions by investigating enlarged regions of parameter space (with special attention paid to the delay and the asymmetry) and further identifies an array of novel effects. The enlarged region is particularly explored in the context of the response of both ON/ON and ON/OFF networks to stimuli (static as well as time-periodic) close to and away from the Andronov–Hopf regime; our previous work was limited to the regime away from the Andronov–Hopf bifurcation. It compares the propensity to oscillate of asymmetric ON/OFF nets to that of symmetric ON/OFF nets and of ON nets. Further, it contrasts the input–output characteristics of such recurrent networks in the time and frequency domains, enabling a comparison of their resonance properties. The paper also presents novel results on a newly found discrepancy between the response of ON cells in the central region (i.e., where external forcing is applied) in ON/ON nets versus ON/OFF nets in the context of periodic input, and exposes the subtle role of asymmetry and of feedback in this effect and in frequency doubling in general. Finally, we study the response of ON/OFF nets to periodic gratings, i.e., periodic forcing in both space and time, and discuss how these results can shed light on certain aspects of frequency-doubling phenomena known to occur in the retina under conditions of periodic spatiotemporal illumination [21, 22].

In Section 3, we review the mechanism by which a static spatially localized pulse triggers global oscillations and investigate the instability threshold as a function of the activity asymmetry between ON and OFF populations. We then study in Section 4 the effect of time-periodic stimulation to see how a lateral response frequency discrepancy is generated and prove that it can only be seen in ON/OFF systems. In each of these cases, we focus on the role played by asymmetrical firing rates in the behavior of neural populations. Lastly, in Section 5, we use the properties of the feedback connections to qualitatively reproduce results on frequency doubling in the retina. Throughout our work, we systematically compare our model predictions based on a neural field formulation with numerical simulations of a network of noisy LIF neurons with all-to-all (i.e., global) delayed feedback.

2 Model

Figure 1 illustrates the neural field model built of ON and OFF cells, connected globally via inhibitory delayed feedback only. Both populations are homogeneously distributed along a spatial domain of size Ω . Activities of the ON and OFF populations propagate to a higher brain center. This center integrates the activity and feeds it back inhibitorily to the sensory layer, i.e., to all ON and OFF cells after some propagation time lag $\tau > 0$. The feedback activity to ON and OFF cells also goes through the same synaptic response function (see below). The parallel sensory pathways of ON and OFF cells are thus identical. The only difference is an interneuronal relay between the external stimulus and the OFF cell, which inverts the polarity of incoming sensory signals. For simplicity, we have omitted the dynamics of any primary sensory receptor cell, as well as the connectivity between these cells and the ON and OFF cells that would determine the receptive field. In the visual system, such primary cells also include many classes of retinal ON and OFF cells, which project to thalamic ON and OFF cells. In contrast, in the electric sense, the receptors are only of the ON type and project to ON and OFF pyramidal cells (known as E and I cells, respectively). No lateral connections between cells are assumed, although spatially localized

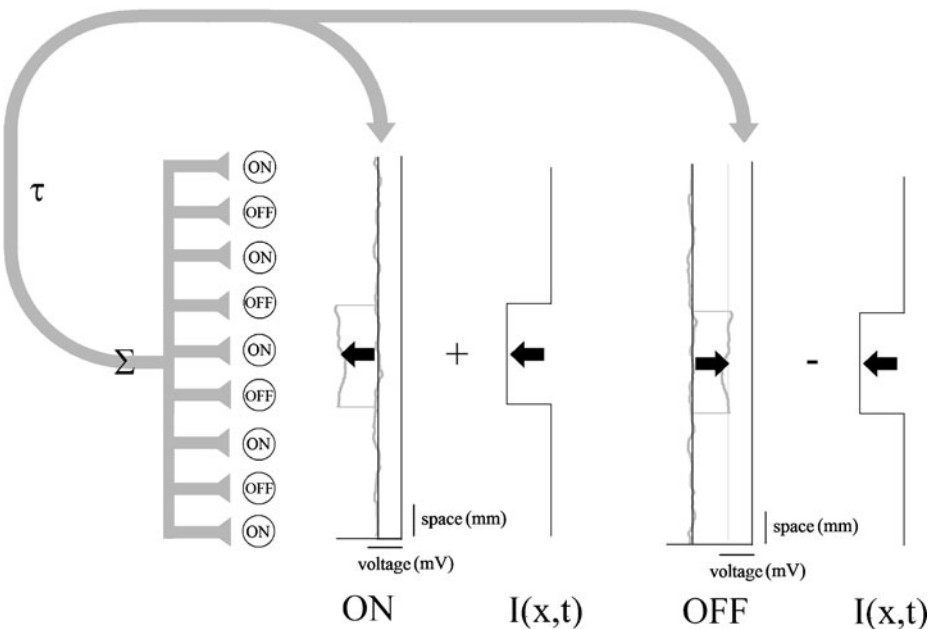


Fig. 1 Schematic of the driven ON/OFF network. The spatial extent of the network is shown vertically, while the mean somatic membrane potential, or activity, across the domain is drawn horizontally. The system is composed of a layer of intercalated ON and OFF pyramidal cells. As an example, here OFF cells (*right*) have a higher activity level than ON cells (*left*). When the input $I(x, t)$ increases and is applied to both cell types, ON cells become more excited, and OFF cells have a reduced activity. All activities are summed (Σ) across the network and sent back to the pyramidal cell layer with all-to-all delayed feedback coupling. Lateral connections between neural sites are considered weak and negligible

sensory stimuli drive localized ON and OFF populations, with direct and inverted polarity, respectively. Local perturbations are nevertheless propagated throughout the network via the recurrent loop, where they generate linear effects, as well as nonlinear effects resulting from bifurcations.

The architecture considered here, although common to many early sensory systems, is inspired by the layout of the electrosensory lateral line lobe (ELL), found in the weakly electric fish, where very few lateral connections exist [23]. This point distinguishes our approach from most neural field models, which typically incorporate spatial kernels. Local circuitry has indeed an important impact on the generation and stability of spatial patterns [24–27], but we focus here on the effects of delayed interactions. Nevertheless, our previous work [28] has shown that moderate instantaneous recurrent connections, mimicking local anatomy, influence only quantitatively the tendency of a dominantly inhibitory delayed feedback system to oscillate by altering the oscillatory response threshold and frequency. These effects have further been shown to not change the dynamics of this model qualitatively. Note that while the model setup is inspired from the electrosensory system, it also applies to any recurrent network in which the cells receiving global feedback can be split into two groups: ones that respond to external input changes with activity changes of similar and opposed polarity.

The mean somatic membrane potential, or *activity*, of the subpopulations $u_{\text{on}}(x, t)$ and $u_{\text{off}}(x, t)$ evolves according to the dynamics

$$\begin{aligned} (1 + a^{-1}\partial_t) u_{\text{on}}(x, t) &= -A(t - \tau) + I(x, t) \\ (1 + a^{-1}\partial_t) u_{\text{off}}(x, t) &= -A(t - \tau) + V_o + sI(x, t), \end{aligned} \tag{1}$$

where a is the time constant of the synapse, whose response to a delta-function spike is of the form $\eta(t) = ae^{-at}$. We will set at $a = 1$ throughout our work. The sensory signal $I(x, t)$ is added to the activity of an ON cell with preserved polarity, while an OFF cell receives the input with inverted polarity ($s = -1$). Also, the OFF cell generally fires at a different rate in the absence of input ($I = 0$) and feedback ($A = 0$); without loss of generality we consider $V_o \geq 0$. We will make comparisons between ON/OFF networks and ON/ON networks. Thus, we parameterize ON/OFF networks by setting $s = -1$ and ON/ON networks by setting $s = +1$. The recurrent feedback term A integrates the activity of each population across the network

$$A(t - \tau) = G \int_{\Omega} dy [\alpha_{\text{on}} f(u_{\text{on}}(y, t - \tau)) + \alpha_{\text{off}} f(u_{\text{off}}(y, t - \tau))], \tag{2}$$

where $f(u) \equiv (1 + e^{-\beta(u-h)})^{-1}$ is a sigmoidal firing rate function, with threshold h and gain β . The network full spatial extent is here $\Omega = 1$ and remains fixed throughout. α_j for $j = (\text{on}, \text{off})$ corresponds to the proportion of j type cells among the total population. These will be fixed at $\alpha_{\text{on}} = \alpha_{\text{off}} = 0.5$, so that our network contains an even number of ON and OFF cells. The feedback gain G will be fixed to 1 for the rest of the analysis. We further set $\beta = 25$, so that our firing rate functions are relatively smooth sigmoids. The feedback is nevertheless a nonlinear function of its input u , which makes the whole system nonlinear. In our comparative study, we frequently present the alternative description provided by a

noisy leaky integrate-and-fire network. The evolution of the membrane potential of the j th LIF neuron obeys

$$\begin{aligned} \frac{dv_j^{\text{on}}}{dt} &= -v_j^{\text{on}} + g \sum_{t_i} \eta(t_i - \tau) + \mu + \xi(t) + I(j, t) \\ \frac{dv_j^{\text{off}}}{dt} &= -v_j^{\text{off}} + g \sum_{t_i} \eta(t_i - \tau) + \mu + \xi(t) + V_o + sI(j, t), \end{aligned} \tag{3}$$

with Gaussian white noise $\xi(t)$ of intensity D , i.e., the autocorrelation is $\langle \xi(t)\xi(t') \rangle = 2D\delta(t - t')$. The feedback gain is denoted by g , the spiking times of all neurons by t_i , and the bias current by μ . V_o is here again the asymmetry parameter. This setup is analogous to the neural field description given in (1), where only mean somatic membrane potentials are taken into account.

3 Responses to static stimuli

The type of response generated by a static (time-independent) sensory input depends on the proximity of the selected parameter set to the Andronov–Hopf curve, which separates equilibrium (fixed point) solutions from oscillatory solutions. There are two cases to consider: the Andronov–Hopf regime and the fixed point regime. The fixed point regime is typically reached by selecting small or zero delays. In this regime, only feedback dynamics provides nonlinear effects in response to sensory driving, although not of the oscillatory type. This case is ideal to examine basic effects of recurrent connections. Larger delays bring the system closer to the Andronov–Hopf regime where intrinsic oscillations emerge. In this case, an increase in a static input will cause a transition to oscillatory activity. Nonlinear properties of the feedback are also present in this region of parameter space, but often difficult to separate from the oscillatory component of the solutions. Below we investigate the dynamical impact of static and spatially nonhomogeneous driving in each of these regimes, by selecting an appropriate small/large delay.

3.1 Oscillatory dynamics

Oscillations appear in inhibitory recurrent systems by increasing the delay or the feedback gain. Steady states of (1) for some time-independent stimulus $I(x, t) = I(x)$ are nonhomogeneous functions, implicitly determined by

$$\begin{aligned} \bar{u}_{\text{on}}(x) &= A(\bar{u}_{\text{on}}, \bar{u}_{\text{off}}) + I(x) \\ \bar{u}_{\text{off}}(x) &= \bar{u}_{\text{on}}(x) + V_o + (s - 1)I(x). \end{aligned} \tag{4}$$

Setting $u_j(x, t) = \bar{u}_j(x) + \tilde{u}e^{\lambda t}$, $\tilde{u} \in \mathbb{R}$, $\lambda \in \mathbb{C}$, yields the characteristic equation

$$\lambda + 1 + Re^{-\lambda\tau} = 0. \tag{5}$$

Andronov–Hopf bifurcations occur for $Re(\lambda) = 0$ with $\lambda = a + iw$, $w \neq 0$, where the parameter R is defined by

$$R = \frac{1}{2} \left[\int_{\Omega} dy f'(\bar{u}_{\text{on}}(y)) + \int_{\Omega} dy f'(\bar{u}_{\text{off}}(y)) \right]. \tag{6}$$

This function corresponds to the amplitude of the linear component of the feedback and thus determines the impact of the feedback term on the steady-state linear stability. It is the first coefficient of the Taylor expansion of A near the fixed point $(\bar{u}_{\text{on}}, \bar{u}_{\text{off}})$. Note that R depends on the response polarity s , since it is a function of the steady states $\bar{u}_{\text{on,off}} = \bar{u}_{\text{on,off}}(s)$. As a result, the eigenvalue dependence on the network type (ON/OFF and ON/ON) is embedded within the last expression. The parameter R is an integral of the steady states over the domain Ω and is maximized when the activities u_{on} and u_{off} are in the neighborhood of the threshold h . Oscillations will be triggered by external inputs that allow steady states $\bar{u}_{\text{on,off}}$ to approach

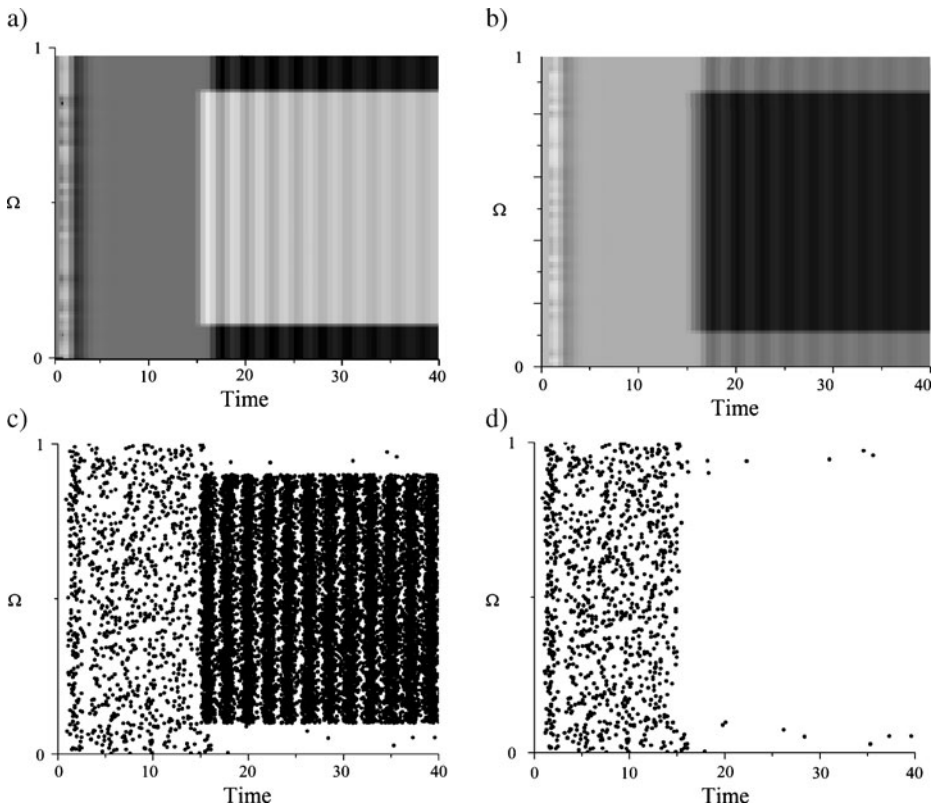


Fig. 2 Localized pulse generating oscillatory activity in an ON/OFF network for both the neural field and integrate-and-fire descriptions. The activity of ON cells is shown on the *left* and of the OFF cells on the *right*. As the input is turned on, the activity of stimulated ON (resp. OFF) cells increases (resp. decreases); the resulting change in the feedback causes a bifurcation. The neural field model (**a**, **b**) shows the ON and OFF populations reaching a stable limit cycle after a short transient. The global oscillations in the LIF model (**c**, **d**), shown in the *lower panels*, take the form of periodic firing rate modulations. Parameters are $I_0 = 0.5$, $V_0 = 0.0$, $\Delta = 0.8$, $h = 0.25$, and $\tau = 0.8$ for the neural field description. The LIF model parameters are $I_0 = 1.9$, $h = 1$, $\mu = 0.4$, $g = -0.07$, $D = 2.0$ for $N = 1,000$ cells with Gaussian white noise; parameters have been scaled to closely match the response frequency in the neural field case. The input has an amplitude I_0 and a width of $\Delta = 0.8$ for $t > 15$. Throughout the paper, we set $\alpha = 1$, $\beta = 25$, and $\Omega = [0, 1]$. Time in the panels is dimensionless. However, we may scale the time axis such that 1 time unit = 10 msec, as the physiologically measured delay range suggests. In this case, the oscillation frequency is close to 50 Hz, and corresponds to the range of frequencies measured in the electrosensory system

h sufficiently closely, such that R crosses the instability threshold $R = R_c$. This critical value is defined by:

$$\tan(\omega(R_c)\tau) + \omega(R_c) = 0. \quad (7)$$

This linear analysis predicts that the frequency of the oscillation right at the Andronov–Hopf bifurcation is $\omega(R) = \sqrt{R^2 - 1}$.

Transitions to oscillatory behavior are a function of asymmetry. These transitions depend on the spatial distribution of the sensory signals. External sensory driving has to generate a sufficient change in the value of R to cause $R > R_c$ and trigger stable oscillations in the whole network, that is, excite or inhibit a sufficiently large fraction of the ON and/or OFF population to activity levels near the feedback threshold h , where R is maximal. The further the activities are from threshold, the larger the input must be to cross the critical value. A typical example of input-driven oscillatory response, occurring via an Andronov–Hopf instability in an ON/OFF network ($s = -1$), is illustrated in Fig. 2. We compare integrate-and-fire and neural field descriptions. The stimulus considered is a pulse, which is defined by $I(x, t) = I_o$ for $x \in \Delta = [x_1, x_2]$ and $t_o < t < t_1$ while $I(x, t) = 0$ otherwise. At the onset of the input, OFF cells are inhibited and ON cells are excited. The resulting excursion of the parameter R across the instability threshold R_c is here caused by the ON cells, whose activity reaches the neighborhood of the threshold h , while the activity of the OFF cells decreases far below. In this example, $V_o = 0$, and thus both ON and OFF populations show the same activity level prior to and after the stimulation. The range of spatial widths $\Delta \equiv |x_2 - x_1|$ and amplitudes I_o triggering stable oscillations in this context have already been established [28]. A question remains: how are transitions to oscillations affected if the spontaneous firing rates are different, i.e., $V_o > 0$?

The asymmetry level between ON and OFF populations increases the response possibilities, as the feedback does not operate in an all-or-none fashion. Without any stimulation, V_o introduces two distinct *effective* feedback thresholds, $h_{\text{on}} = h$ and $h_{\text{off}} = h + V_o$, causing two possible Andronov–Hopf transitions in parameter space. This phenomenon can be seen in Fig. 3 which shows the regions in (τ, h) -parameter space where oscillations are stable, for different levels of asymmetry and without any input, i.e., $I(x, t) = 0$. As V_o increases, the stable domain splits into two regions, corresponding to the predominant response of either ON or OFF populations and according to the new effective thresholds. This steady-state property of the system illustrates that transitions to stable oscillations occur within two regimes, as a consequence of different effective ON and OFF feedback activation thresholds. A positive pulse moves the activity of ON and OFF cells toward critical levels, located at h_{on} and h_{off} , around which the value R increases significantly.

A brief comparison between ON/ON and ON/OFF net responses (i.e., the cases $s = +1$ and -1) with respect to the proximity of the Andronov–Hopf regime has been presented in [20]. There, it has been shown that input-driven oscillatory activity is more prevalent in ON/ON nets. However, the presence of asymmetrical firing rates, i.e., $V_o \neq 0$, is expected to significantly alter this result. Figure 4a shows the effect of an increasing asymmetry V_o on the ability of a pulse of amplitude I_o to trigger stable oscillations. This is shown for both network configurations. This complex structure represents points in parameter space for which $R > R_c$. It becomes quite hard to give an intuitive interpretation of what is going on, given the complex forms of the oscillatory zones, but we may still state the general results.

For V_o small, asymmetrical firing rates have a radically different impact on ON/OFF and ON/ON network responses. In the ON/ON case, there is an oscillatory response sensitivity shift toward inhibitory signals, while the opposite occurs for ON/OFF configurations.

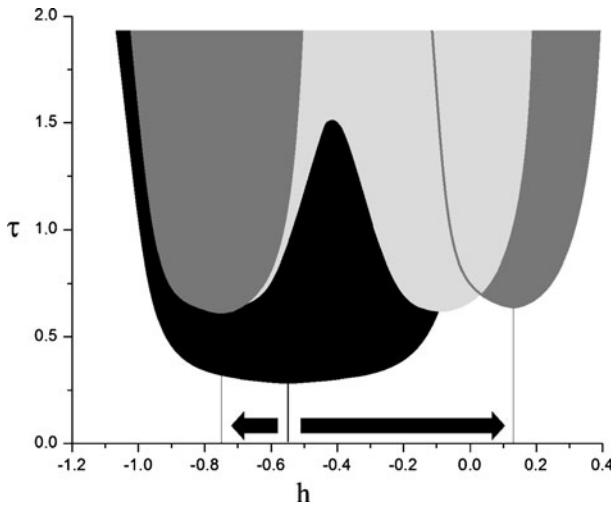


Fig. 3 Regions in the (τ, h) subspace of parameter space where global oscillations are stable for $I(x, t) = 0$ and various asymmetry levels (adapted from [20]). For $V_o = 0$ (*black-shaded region*), ON and OFF populations share the same spontaneous firing rates and thus have the same activity relative to the feedback threshold. The resulting Andronov–Hopf region has the shape of a parabola, as in an ON/ON system. If V_o is increased to 0.2 (*gray-shaded region*), the stable domain starts to split into two distinct regions, showing that ON and OFF populations do not have the same activity level with respect to the threshold of the system and thus that their relative Andronov–Hopf domains (where cyclic solutions becomes stable) are becoming distinct. The separation becomes even more appreciable with respect to initial case when V_o reaches the value of 0.4 (*dark gray-shaded region*) as indicated by the *black arrows*. Parameters are as in Fig. 2 with $I(x, t) = 0$

Given a broader interval of inputs causing oscillation, these are more prevalent in ON/ON networks for the weakly asymmetrical cases $V_o \lesssim 0.15$. This confirms the property of our two-population system: *ON/OFF nets have symmetrical behavior w.r.t. excitatory and inhibitory inputs, while ON/ON nets do not*. This result holds over a large range of asymmetry values; beyond this, the ON/ON configuration surprisingly starts to respond to both input polarities with oscillations, as one can see in Fig. 4c. Further, the opposite occurs in the ON/OFF case, where the system no longer responds to both polarities. We emphasize that these results are dependent on the input spatial width. Larger pulses are responsible for greater variations of the parameter R , which implies that smaller amplitudes are required to reach the oscillation threshold R_c .

3.2 Steady-state dynamics

For small delays, a static input does not trigger an oscillatory response. This is because the threshold R_c exceeds the maximal bound of (6). Nonlinear effects are nevertheless generated through the interaction of the input with the feedback, since ON and OFF populations activate the recurrent connections differently depending on their activity prior to receiving input. Spatially localized pulses, in particular, are ideal to study these effects, as the sharp spatial separation between stimulated and nonstimulated sites emphasizes feedback dynamics. The system may then display distinct activity patterns inside (central) and outside (lateral) the pulse. Previous studies [20] of central/lateral discrepancies in ON/OFF nets were

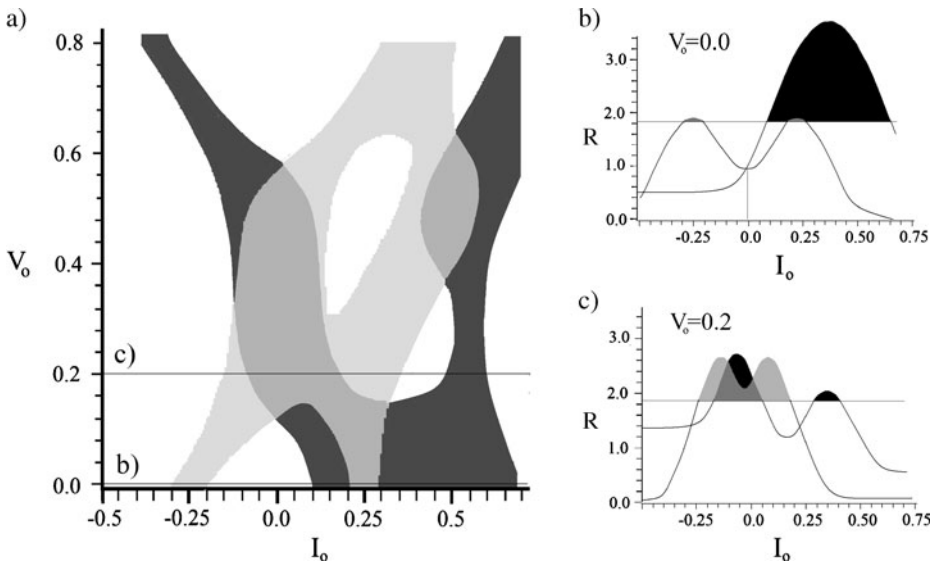


Fig. 4 **a** Regions in (I_o, V_o) space where oscillatory response occurs, for ON/ON (dark gray) and ON/OFF (light gray) network configurations. These points are such that $R > R_c$ in each case. For small asymmetry values, the ON/OFF configuration can respond to both excitatory and inhibitory inputs, the oscillatory response region being symmetrical with respect to the vertical line $I_o = 0$. ON/OFF nets can oscillate for both positive and negative inputs. ON/ON nets have a larger interval of I_o values that cause oscillation compared to ON/OFF nets. An ON/ON net can oscillate in response to both positive and negative inputs only if V_o is large. **b** Slice of the graph shown in **a** for $V_o = 0.0$, illustrating how the parameter R in (6) changes as a function of I_o . Shaded areas correspond to the parameter sets such that $R > R_c$. **c** For larger asymmetry $V_o = 0.2$, an ON/OFF net now has a larger range of inputs that cause oscillations, and ON/ON nets now show two distinct intervals of input amplitudes. Parameters are $R_c \approx 1.83$, $\tau = 1.4$, $\Delta = 0.6$, $h = 0.1$

not compared to ON/ON networks, nor explored as a function of asymmetry. This is our task here.

We consider the case of equal spontaneous activities $V_o = 0$, in which both ON and OFF cells are subthreshold. We focus again on spatially localized stimuli. We also focus on the differences between the activity of both cell types in stimulated regions and nonstimulated regions; this difference is likely important for decoding at a higher level. Static positive inputs locally increase (resp. decrease) the activity of the ON (resp. OFF) cells. The resulting response curve is monotonic (not shown). As the input increases further, so does feedback, leading in both ON/OFF and ON/ON cases to a lateral decrease in activity. ON/OFF systems will have the same global network response for inhibitory inputs, while ON/ON systems, in contrast, will not show any modulation of the feedback.

For asymmetrical cases $V_o > 0$, the response of OFF cells allows the system to modulate the polarity of the response as a function of the stimulus amplitude. Central/lateral responses to an excitatory localized pulse in the fixed point regime are shown in Fig. 5. OFF cells, here maintained at supra-threshold activity because $V_o \neq 0$, are locally inhibited by the incoming pulse, reducing the feedback and thus generating a global increase in activity. If the input amplitude increases, ON cells locally reactivate the feedback amplitude by crossing the threshold, now leading to a global decrease in activity. In contrast, in the case where no OFF cells are present, the only consequence of increasing the stimulus amplitude is an increased feedback inhibition. Consequently, our analysis predicts that

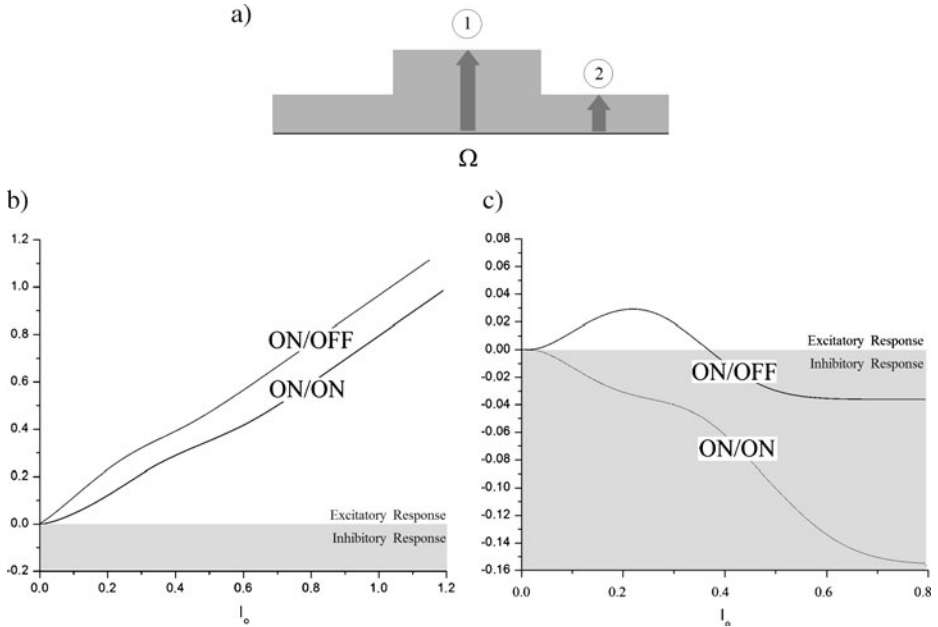


Fig. 5 Central and lateral responses to a spatially localized pulse of amplitude I_0 and width $\Delta = |x_1 - x_2|$ far from the Andronov–Hopf regime, for both ON/OFF and ON/ON network configurations. ON/OFF net lateral response is nonmonotonic, while it is not so in the ON/ON case. **a** Local regions correspond to the neural sites located inside the pulse, i.e., for $x \in [x_1, x_2]$, which are directly stimulated. Lateral sites do not receive the input but are driven only by the feedback. **b** The activity differences between stimulated and nonstimulated states are plotted versus I_0 . The central response is monotonic for both configurations, although two slopes distinguish the curves. **c** Lateral responses are radically different for ON/ON and ON/OFF nets. The ON/OFF response to the pulse is nonmonotonic as a function of pulse height I_0 , while the ON/ON response is monotonically decreasing. The difference between the curves in **b** and **c** is I_0 in both cases. Parameters are $V_o = 0.3, h = 0.05, \tau = 0.2$

ON/OFF systems exhibit nonmonotonic lateral response curves, while ON/ON systems are restricted to inhibitory lateral responses. Note that these steady-state effects at small delays, caused by input–feedback interactions, are also at work in the larger delay regime of the previous section. There, they influenced the distance to threshold and thus transitions to oscillations caused by static inputs, but their role is somewhat masked by these more dramatic transitions to oscillatory activity.

Finally, we note that some ON and OFF cells respond to steady input currents by showing bursts of spikes at the onset and offset of stimulation—thus lending another meaning to an “off response” cell. These transient effects have been linked to various neural mechanisms like post-inhibitory rebound in many sensory systems (see [29]) where they play an important functional role. They are typically reproduced by models in which the neuron state is dependent on the time derivative of the input, where sudden changes in the input temporal structure result in important membrane voltage changes. We have not yet drawn attention to the fact that recurrent connections do reproduce similar responses under certain conditions. For example, in [20], Fig. 7, both ON and OFF cells outside the stimulation zone exhibit a sudden increase in activity at both onset and offset of the pulse. In our model, the effect is most pronounced for lateral cells and is a consequence of the

nonmonotonic response shown in Fig. 5—which itself is a consequence of the asymmetry $V_o \neq 0$. Central units do not show this behavior as clearly, as the amplitude of this excursion is relatively smaller than the amplitude of the stimulus itself. The effect is nevertheless present as a gentle slope change exists in the response curve. Thus, the variety of transient on and off responses seen experimentally in a variety of systems may in some cases have a contribution from feedback effects.

4 Time-periodic stimuli

Oscillations in neural systems can also be triggered by time-periodic stimuli. Such nonautonomous components of the input determine the main features of the system’s response, but additional nonlinear effects can be generated via the recurrent interactions. Nonautonomous problems, however, pose an important analytical challenge, as dynamical system theory has few tools to determine the shape and stability of the resulting nonstationary solutions. Results have nevertheless been obtained for specific input shapes, like linear ramps [30], laterally drifting bumps [31], and global periodically forced spiking models [32]. In our context, the absence of a spatial kernel simplifies the analysis greatly, as the dynamics can be essentially described by the interaction between the stimulus and its “image” propagated via feedback. We thus analyze the response patterns close to and away from the Andronov–Hopf regime by selecting the appropriate delay.

In Fig. 6, we show the response of ON cells to a spatially localized pulse with a sinusoidally modulated amplitude, in both ON/ON or ON/OFF network configurations. Two main results are obtained when one analyzes in detail the distinction between these two responses: (1) second harmonic or frequency-doubled response (laterally) and (2) sustained amplitude response (centrally). We will analyze each of these cases separately.

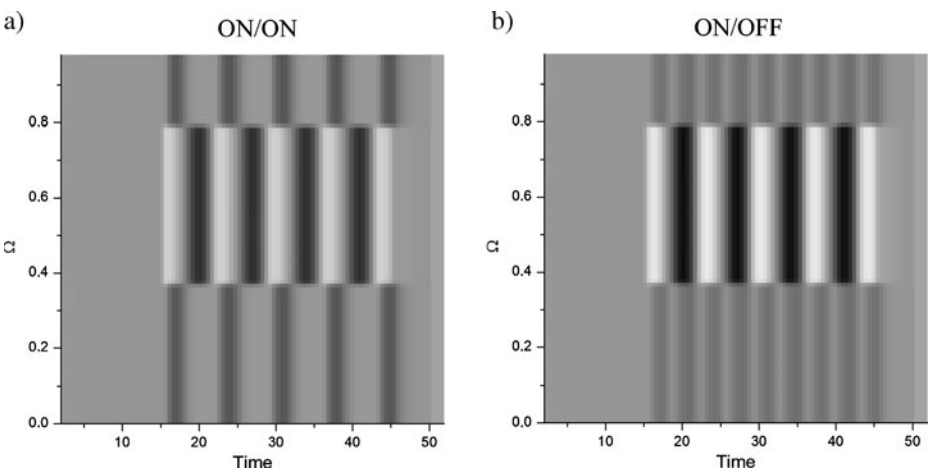


Fig. 6 ON cell response to a sinusoidally modulated localized pulse. **a** The ON/ON response is characterized by a central response in phase with the input, while the lateral response is antiphase with respect to the central response. **b** The ON/OFF response exhibits a lateral frequency-doubling effect, where the activity oscillates at twice the input frequency, while centrally the activity is in phase with the input and oscillates at the driving frequency. Furthermore, the amplitude of the central response is higher than in the ON/ON case. Parameters are $\Omega = 1$, $\tau = 0.3$, $h = 0.0$, $I_o = 0.5$ for $x \in [0.35, 0.75]$ and $t > 15$, $w_o = 0.9$, $V_o = 0.05$

Further, in this section, we restrict our analysis to inputs which possess the following spatiotemporal structure: $I(x, t) = I_o \sin(\omega_o t)$ for $x \in \Delta = [x_1, x_2]$ and $t_o < t < t_1$ while $I(x, t) = 0$ otherwise.

4.1 Frequency doubling

Lefebvre et al. [20] showed that periodic driving, in the case of small delays, results in a lateral frequency-doubling effect in ON/OFF networks. This effect is caused by the combined responses of ON and OFF populations, resulting in the feedback being modulated at twice the input frequency. Underlying this effect is the fact that the recurrent feedback loop acts as a full-wave rectifier, getting a boost from both positive and negative going phases of the input. This effect was found in ON/OFF nets; here we contrast it with the behavior of an ON/ON net with similar forcing. We further show that it can occur in a LIF network. Our aim is to characterize the functional differences between this type of behavior, which appears to be specific to ON/OFF networks, and the antiphase lateral response seen

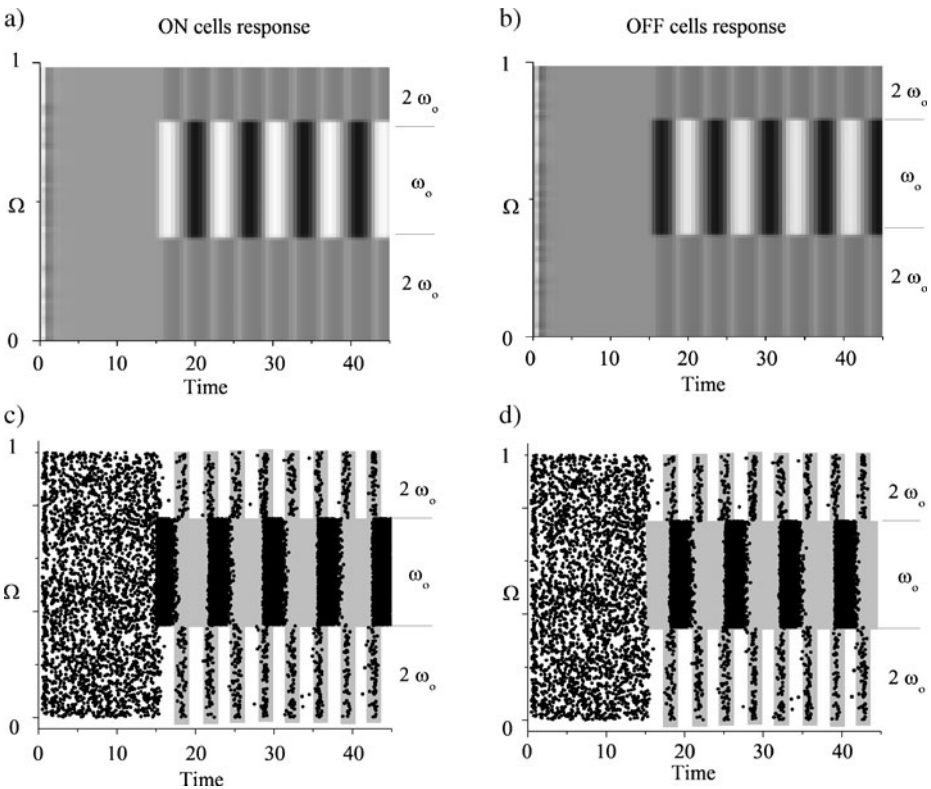


Fig. 7 Sinusoidally modulated localized pulse generating a lateral frequency-doubling effect in an ON/OFF net. ON and OFF population responses are presented, for both neural field (a, b) and spiking (c, d) approaches. The parameters for the neural field description are identical as in Fig. 6 while for the LIF description, these are $\tau = 0.3$, $h = 1$, $I_o = 5.5$, $\mu = 1.05$, $V_o = 0.05$, and $g = -0.06$ for Gaussian white noise

in ON/ON networks, as seen in Fig. 6. Further here, we explore the effect of increasing delay times on the structure of the response. As a result, this problem must be considered both close to and away from the Andronov–Hopf regime.

Away from the Andronov–Hopf bifurcation in the fixed point regime, when the delay is small, the input cannot trigger a bifurcation as the spectrum of eigenvalues is bounded to the left of the imaginary axis. As Fig. 7 shows for both the neural field and LIF models, ON and OFF populations respond to localized signals with opposed polarity. In the case of sinusoidally modulated amplitudes, the reversed OFF response constitutes an antiphase (i.e., 180° phase shifted) image of the signal transmitted to the ON cells. The combined responses of ON and OFF cells result in a signal oscillating at twice the input frequency.

Frequency doubling might be explained when one looks at the interaction of the ON and OFF cell activity with the feedback activation threshold h . Figure 8a illustrates the sequence of events leading to feedback oscillations. Before the stimulus is applied, steady firing rate states are reached by both ON and OFF populations. As the sinusoidally modulated pulse is turned on at $t = t_1$, $I(x) > 0$ for $x \in [x_1, x_2]$, and ON cell activity increases until the feedback activation threshold is met. This increases the amplitude of the feedback, resulting in a lateral decrease in activity. As the first half of the input cycle ends and where $I(x, t) \approx 0$, the ON population decreases its activity below the threshold, which deactivates the feedback. The activity then increases laterally. Now OFF cells become excited, due to their reversed response, and activate the feedback again. The lateral activity decreases once more. This sequence of events is not instantaneous, and the lateral response shows two small bumps of activity for every input period, caused by two feedback activation/deactivation sequences. This process repeats itself until the input is turned off. The resulting lateral activity behavior corresponds to the time evolution of the feedback term $A(t)$, which oscillates at twice the input frequency.

Of particular significance is that our analysis predicts that lateral double frequency responses are only possible when ON and OFF populations are present. As Fig. 8b illustrates, ON/ON type networks do not exhibit this behavior. This is because ON/ON

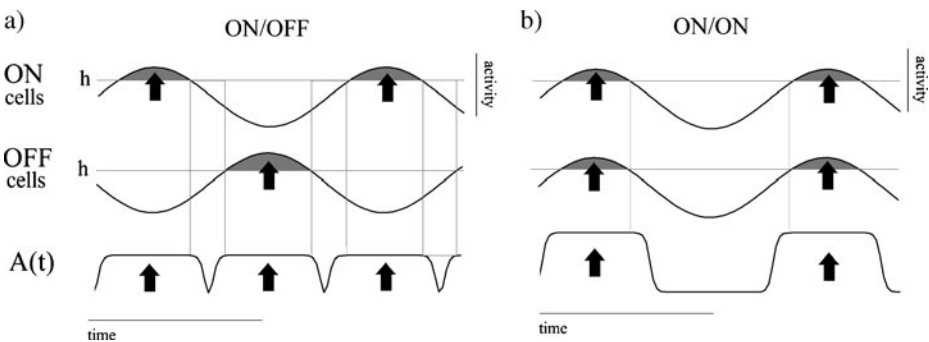


Fig. 8 Schematic representation of the time evolution of the activity of cells in ON/OFF and ON/ON nets. **a** As the activity of either ON or OFF cells increases beyond the threshold h (shaded areas), the amplitude of the feedback increases. In ON/OFF nets, stimulated ON and OFF cells never activate the feedback simultaneously; the resulting recurrent signals oscillate at twice the input frequency. **b** Stimulated cells in an ON/ON net activate the feedback simultaneously, which then oscillates with the same frequency as the input. The profile of the feedback term $A(t)$ as in (2) is also shown in the two cases

systems only activate and deactivate the feedback once per input cycle. The lateral response then corresponds to a sequence of steady activity plateaus, corresponding to successive feedback changes in amplitude caused by ON cells reaching the threshold. The resulting

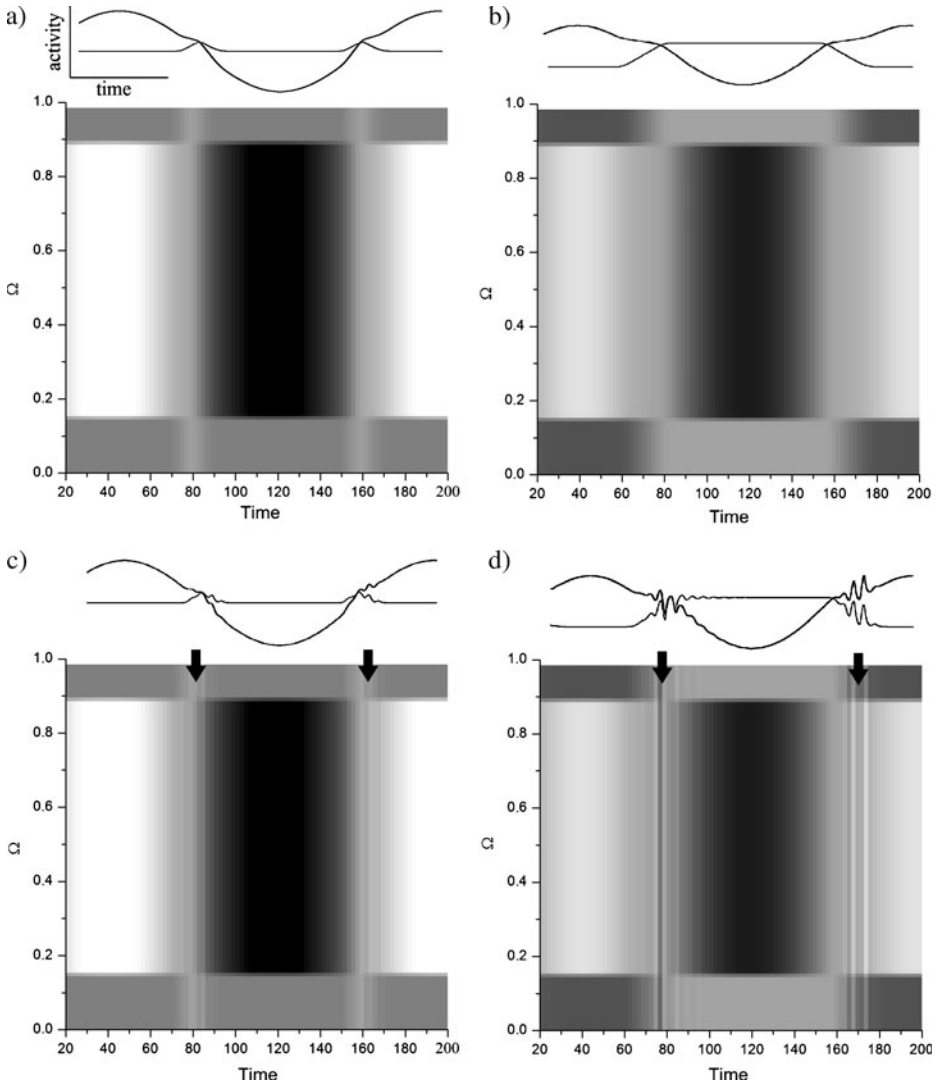


Fig. 9 ON cell responses to a time-periodic stimulus in ON/OFF and ON/ON nets, far from (a, b) and close (c, d) to the Andronov–Hopf regime. Andronov–Hopf cycles appear whenever ON or OFF cell activity is near the feedback threshold h , making the parameter R cross the critical value R_c . A small frequency of $w_o = 0.04$ allows those cycles to gain sufficient amplitude to be seen. The ON/OFF net is shown on the left (a, c) and ON/ON on the right (b, d). On the top of each panel, bold lines describe the central temporal evolution of the solutions, while thin lines describe lateral dynamics. Other parameters are $\Omega = 1$, $I_o = 1.1$ for $x \in [0.15, 0.85]$ and 0 elsewhere, $V_o = 0.05$ and $h = 0.0$. The delay chosen in the fixed point regime is $\tau = 0.5$ while $\tau = 1.8$ near the Andronov–Hopf regime

effect is a central–lateral response phase shift of 180° . One might characterize the response of ON/OFF networks by comparing the input contrast curves generated by this configuration to those for the ON/ON systems. Frequency doubling and lateral phase shift can be seen as outcomes of global feedback driving but are seen predominantly in regions where the input has smaller or zero amplitude.

Figure 9a, b shows the central and lateral responses for small delays. In the case of large delays, a similar behavior occurs, but the input makes the parameter R cross back and forth over the critical value R_c . For large delays, R_c is also much smaller. As we can see from Fig. 9c, d, the variations of R generate periodic epochs of Andronov–Hopf cycles, or bursts, superimposed on the activity profile provided by the input. This makes the network response look even more nonlinear. The temporary transitions to oscillatory activity are caused by the activity levels getting closer to and farther away from the threshold h , changing the value of R accordingly.

In an ON/OFF configuration (Fig. 9c), only one stimulated population at a time approaches h , as explained in Fig. 8. The variation of R is thus much smaller than in the ON/ON case, where the two populations simultaneously interact with the feedback. The excursion of the parameter R in the ON/OFF case takes place in the vicinity of the bifurcation, causing relatively small oscillations. In contrast, oscillations in the ON/ON case are much larger, as the excursion of the parameter R takes place further into the Andronov–Hopf regime. We note that this effect is apparent mainly for small input frequencies, as the stimulus has enough time to gain the required amplitude to generate a bifurcation.

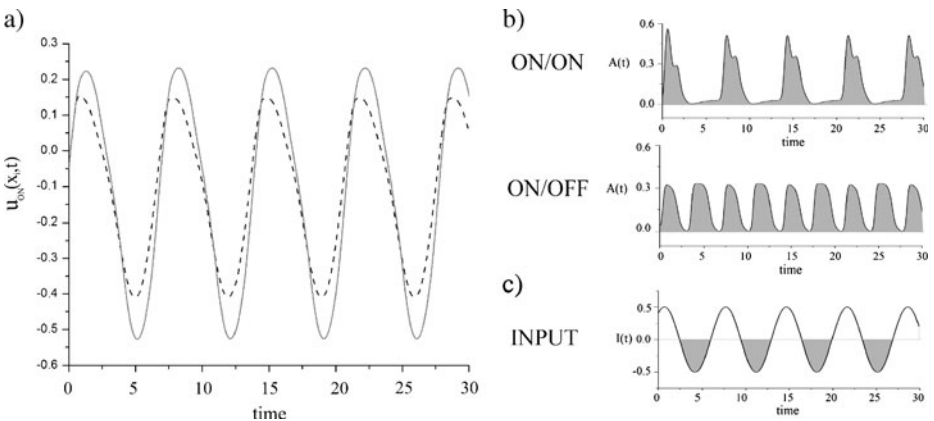


Fig. 10 Response amplitude discrepancy of central ON cells in ON/ON and ON/OFF networks. **a** Evolution of the activity of sinusoidally driven ON cells, for central locations, i.e., $x_i \in \Delta$. Activity oscillations in an ON/OFF network (*solid line*) are larger than in an ON/ON network (*dashed line*). **b** Resulting evolution of the feedback $A(t)$ according to a sinusoidal stimulus, in the ON/ON and ON/OFF cases. In the ON/ON case, the sudden activation of the feedback caused by the two populations is such that $A(t)$ makes high amplitude excursions away from the resting value, resulting in a strong inhibitory effect on the network. This decreases the amplitude of the response, but only when the amplitude of the input is positive. In the ON/OFF case, the simultaneous and antiphase responses of ON and OFF cells result in a full-wave rectification across the feedback loop. The variations of the feedback amplitude are much smaller, meaning that less inhibition affects the response at the sensory layer. Further, the activation of the negative feedback by the OFF cells during the negative components of the input results in an amplification of the response. The input temporal structure is plotted in **c**. Parameters are $\Omega = 1$, $\tau = 0.3$, $h = 0.0$, $I_0 = 0.5$ for $x \in [0.35, 0.75]$ and $t > 15$, $w_o = 0.9$, $V_o = 0.05$

4.2 Amplitude of sustained ON/OFF response

We now consider the amplitude of responses to periodic forcing. The behavior illustrated in Fig. 6 also puts forward another novel effect, namely a central response amplitude difference between purely excitatory networks and those built of both ON and OFF cells. Indeed, the central response of the ON cells has significantly greater amplitude in an ON/OFF setup. This behavior can be explained when one considers the temporal structure of the feedback in the ON/ON and ON/OFF cases. Figure 10a illustrates the central response patterns in both configurations, as well as the feedback time course $A(t)$ as in (2b) when a sinusoidal input is present (which is also plotted in panel c).

In an ON/ON network, whenever the input amplitude increases, both populations recruit the feedback simultaneously, which results in a sudden and high amplitude increase of $A(t)$. The resulting strong inhibitory signal reduces the amplitude of the cell’s response. As the input amplitude then decreases, both populations reduce their activity below the threshold, resulting in a sudden and complete deactivation of the feedback. The remaining negative part of the input is not altered by the feedback, which is not activated.

In an ON/OFF network, however, the feedback $A(t)$ does not reach as high an amplitude because only one population at a time, either ON or OFF cells, can recruit recurrent connections. As the input amplitude increases, only ON cells activate the feedback, resulting in a relatively smaller inhibitory signal. This allows the response of the stimulated ON cells to reach higher amplitudes than in the ON/ON case. And as the amplitude of the stimulus becomes negative, *the negative feedback acts as an amplifier and sustains the response of the stimulated cells*. This is because the negative part of the input makes the OFF cells activate the feedback once again: the feedback amplifies the cellular response.

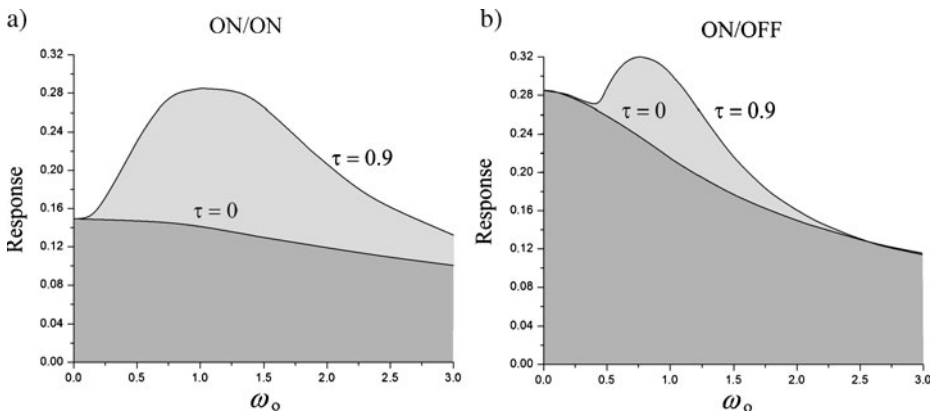


Fig. 11 Response amplitude of central ON cells in ON/ON and ON/OFF nets as a function of input frequency. A sinusoidally modulated pulse of fixed amplitude $I_o = 0.25$ and width $\Delta = 0.4$ generates distinct frequency tuning properties if the system incorporates OFF cells. **a** For $\tau = 0$, ON/ON net response is relatively constant over the range of frequencies considered. The units recruit the feedback pathway, which in turn reduces the amplitude of the cells’ response. For $\tau = 0.9$, the curve shows the resonance due to the Andronov–Hopf frequency. The response amplitude diminishes as the frequency becomes larger because the input becomes too fast compared to the system’s dynamics. **b** In ON/OFF nets, the response curve is lowpass. For $\tau = 0$, the response is maximal at low frequencies due to the feedback amplification, whereas the amplitude is larger compared to the case shown in **a**. Increasing the delay to $\tau = 0.9$ makes the system closer to the Andronov–Hopf regime: a resonant peak becomes visible near the Hopf frequency

The response amplitude deviation shown in Fig. 10 further shapes the frequency tuning properties of ON/ON and ON/OFF nets. In Fig. 11, the response amplitude of driven units is plotted with respect to stimulus frequency for small and large delays. Panel a shows that ON/ON net response is bandpass. For zero delays ($\tau = 0$), the response curve is flat over the range of input frequencies. Increasing the delay to a higher value ($\tau = 0.9$), the resonance peak appears as the system gets closer to the Andronov–Hopf regime and exhibits stronger oscillatory behavior near the characteristic Hopf frequency. In the ON/OFF case (plotted in panel b), the response is lowpass, where stimuli with smaller frequencies trigger responses of amplitudes much larger than in the ON/ON case. If the feedback delay is changed from $\tau = 0$ to $\tau = 0.9$, the Andronov–Hopf resonance peaks appear.

5 Application to sensory systems

The model under study here, which incorporates ON and OFF populations with global recurrent connections, can shed light on recent experimental findings, in both the electrosensory and visual systems. These two systems use ON and OFF cells to integrate sensory inputs and incorporate feedback. We show (1) that some experimental data are reproduced by our generic model, thus providing a simple caricature of the dynamics at work when both populations operate together, and (2) that known results obtained in ON/ON networks still hold when more realism is put in the models by incorporating OFF cells.

5.1 Electrosensation

The electrosensory system is endowed with ON and OFF cells, known, respectively, as E and I pyramidal cells. These cells receive direct input from primary sensory neurons, the electroreceptors, which cover the body of the animal. It is known that E and I cells project back to themselves via the nucleus preeminentialis (nP) after a minimal delay of approximately 10 ms [23]. It is also known that stochastic inputs in time cause oscillatory activity in the gamma band (around 40 Hz) when the inputs are strongly correlated in space [11, 33]. In the context of our model here, spatial correlation is proportional to the number of neurons receiving common input. No such oscillatory activity was seen when neighboring patches of electroreceptors receive independent stochastic forcing. This experimental result was reproduced by computational modeling of a network of E cells projecting to themselves with inhibitory delayed feedback of the type considered here. This was the case for LIF type nets with intrinsic noise driven by external correlated noise [33] as well as for a linear fluctuation theory using stochastic LIF neurons with delayed feedback [11, 34]. The outstanding question is whether the inclusion of OFF cells known to be present in approximately equal numbers as ON cells can alter our understanding of this picture.

In [20], we showed that ON/OFF networks can also oscillate when a sufficient number of neurons receive a static input, enabling the parameter R to cross the critical value R_c . Further, we showed that the range of inputs that cause this transition was more limited than for ON/ON nets. While the deterministic localized “step input” stimulation used in that paper (and here) differs from the stochastic zero-mean stimulus used in [11, 33], the lower propensity of the ON/OFF network to oscillate when an input bump is applied suggests that OFF cells could counteract the genesis of gamma oscillations. However, that result was obtained for a symmetric network ($V_o = 0$). Our new results here for the asymmetric case now show that the situation is more complex. The ability to oscillate really depends on V_o

(see Fig. 4). In some cases, the ON/OFF network may in fact have a greater propensity to show an oscillatory response to a static input. This question could be ultimately settled by determining the spontaneous activities, which can be done by opening the feedback loop surgically or temporarily using pharmacological agents. So it may be that the oscillations seen experimentally in the electrosensory system were in fact supported and maybe even strengthened by the presence of the OFF cells.

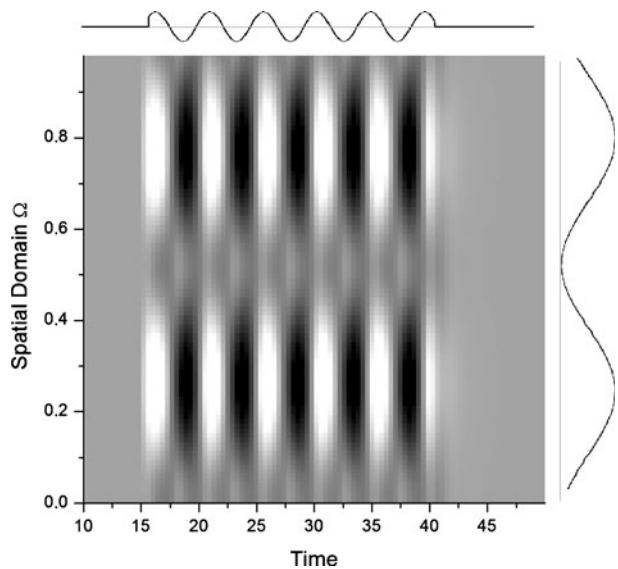
5.2 Response to periodic grating and retinal frequency doubling

In this section, we consider the response of our recurrent network of ON and OFF cells to forcing that is periodic in both space and time. This type of forcing is common in research on the visual system, where it is referred to as contrast-reversed periodic stimulation. For simplicity, we consider sinusoidal gratings. Note, however, that we do not consider sinusoidal drifting gratings which are also often used in vision research (we only comment briefly on the resulting dynamics below). Here, the modulation is fixed in space. Hence, there is a discrete set of points in space, at the local minima of the spatial modulation, that never receive any stimulation beyond the background stimulation on which the periodic grating is applied. Parameters of this stimulation are the spatial frequency, the temporal frequency, and the spatial and temporal modulation amplitudes, which can be combined into one amplitude factor I_o :

$$I(x, t) = I_o \sin(w_o t)[1 + \cos(\gamma x)] \tag{8}$$

where w_o is the temporal frequency and γ is the spatial frequency. The response of our one-dimensional array of ON cells to the sinusoidal grating is shown in Fig. 12. The temporal part of this forcing, turned on at $t = 15$, is shown above the plot, while the spatial part is shown to the right. This setup is similar to that studied in Section 4.1 on

Fig. 12 Frequency doubling caused by a spatially and temporally sinusoidal input, mimicking an illumination grating stimulus. This input is presented here to a one-dimensional retina. Parameters are $\Omega = 1$, $\tau = 0.4$, $h = 0.0$, $I_o = 0.5$, $w_o = 1.3$, $V_o = 0.05$, and $\gamma = 13.0$



periodically modulated pulses, except that here the pulses have a sinusoidally repeating profile in space. The activity in the regions receiving more illumination is seen to oscillate at the temporal driving frequency w_o . On the other hand, the activity of regions receiving less illumination are found to oscillate at twice the input frequency even though the input is weak in those regions. The frequency-doubling effect is maximal at positions $x_n = (2n + 1)\pi(\gamma)^{-1}$ where $I(x_n, t) = 0$. The frequency doubling observed here occurs because the combined responses of ON and OFF populations propagate back through the network via the recurrent connection. Illuminated locations oscillate predominantly at the input frequency, even though the frequency-doubled component is globally driving the system via the feedback—this latter component is just weaker than the direct driving frequency component in the illuminated region. The relative strength of the fundamental and frequency-doubled components thus changes in a continual manner from regions of zero illumination to regions of maximal illumination from the grating.

The addition of OFF cells to our recurrent sensory pathway may be used to shed some light on phenomena occurring in the visual system. Frequency doubling has been observed in many experimental studies of retinal ganglion cells responding to periodic illumination gratings (see [22] and references therein). These observations have also been reproduced computationally [21]. In [22], experiments were carried out in guinea pig retina, where both ON and OFF pathways are present. Lateral responses (outside the illuminated bars) at twice the stimulus frequency were reported and attributed to the presence of nonlinearities in the ON and OFF pathways and to the dimension of the receptive field of amacrine cells. In the experiments, illumination grating stimuli were drifted or reverse-contrasted periodically in time, while the activities of central (sites of maximal illumination) and lateral (position of zero illumination) ganglion cells were simultaneously recorded and compared (see [22] for details). For gratings with a low spatial frequency, the activity was shown to track the input temporal modulation in regions of maximal illumination (labeled “F1” behavior). In contrast, in regions of zero illumination, the activity of the ganglion cells oscillated at twice the temporal input frequency (labeled “F2” or “nonlinear” behavior). In [21], this phenomenon has been reproduced by a complex computational model of a retinal subcircuit in which frequency doubling, also called “second harmonic response”, has been linked to photoreceptor nonlinearities and amacrine wide-field effects. The model, developed for the ON pathway because the data on the OFF pathway are more scarce, includes the properties of subtypes of photoreceptors, horizontal cells, bipolar cells, ganglion cells as well as two classes of amacrine cells: narrow field (“nested” amacrine cells) and wide field amacrine cells. The complex wiring diagram involves feedforward inhibition and recurrent negative feedback loops.

The setting of the experiment described in [22] and the work in [21] suggests that our model might be used to reproduce certain features of the observed dynamics. Those authors state that F2 nonlinear responses—qualitatively similar to our lateral frequency-doubling behavior—are due to the ganglion cell’s “nonlinear” receptive field, which possesses quite distinct spatial summation properties in comparison to the more familiar center-surround “linear” receptive field. F2 responses are not sensitive to the recording position within the spatial grating and thus do not appear to be determined or influenced by local spatial connectivity. While the F2 responses are constant over all grating phases, the F1 responses (due to the standard center-surround receptive field) are proportional to the illumination in the grating. This is qualitatively similar to what is seen in Fig. 12.

Further, the F1 and F2 responses show similar dependencies on the spatial frequency of the grating, and this dependency is preserved over the receptive field of the ganglion

cells. Also, the authors of [22] report that nonlinear receptive field effects are caused by the spatial summation of independent “subunit” responses that populate a wide area around the ganglion cell’s dendritic field. The range of these connections is supposedly a consequence of the presence of wide-field amacrine cells. As a result, F2 responses measured across the receptive field were shown to sum up linearly at the ganglion cells.

Thus, the interplay of the activation of ON and OFF cone pathways involves weakly interconnected subunits distributed across the receptive field. Their activity is integrated via the wide-field amacrine cells, which is analogous to a large-scale feedback pathway with weak lateral connectivity, as in our model and in the ELL discussed in Section 5.1. Thus, although retinal subcircuits are not spatially homogeneous and our model lacks the complexity to reproduce the full range of phenomena described in [22], we argue that the qualitative behavior of the nonlinear responses of ganglion cells to a periodic grating can be reproduced without spatial connectivity considerations, by including globally summed inhibitory effects. In this context, our model proposes a mechanism which is responsible for input rectification, which relies on the nonlinearity of both the ON and OFF recurrent pathways.

We have considered here only contrast-reversed gratings, as opposed to drifting gratings. Preliminary results with drifting sinusoidal gratings do not reveal frequency doubling in our one-dimensional array (not shown). The difference with the retinal data under these conditions may be due to the fact that two dimensions are needed to reproduce the basic observations or that more intricate circuitry has to be included. Also, the frequency doubling exhibited by our model is not sensitive to the spatial frequency of the contrast-reversed grating, which is also the case for the data over a certain range of spatial frequencies. But at some point, the lateral connectivity and other details of retinal circuitry do set a spatial scale beyond which the effect decreases until it is no longer seen.

6 Conclusion

In this paper, we analyzed the main differences between the sensory processing capabilities of networks built of ON and OFF cells (ON/OFF) with networks built of ON cells only (ON/ON). We have shown that both types of nets integrate spatiotemporal inputs differently. In the context of oscillatory responses reached via Andronov–Hopf bifurcations, symmetric ON/ON systems are more sensitive in the sense that they undergo Andronov–Hopf bifurcations with pulses of smaller amplitude and spatial widths; however, this transition is only allowed for positive inputs. In symmetric ON/OFF systems, the transition occurs on a narrower interval of input widths and amplitudes but is observed for inputs of both positive and negative polarities. This situation changes with the degree of asymmetry in the spontaneous firing rates, controlled by the parameter V_o . We found that the asymmetry greatly influences the bifurcation properties of the system and the propensity to respond to static step inputs with oscillations.

In the context of time-periodic inputs, we demonstrated that only ON/OFF systems exhibit lateral frequency doubling, while ON/ON systems instead show antiphase lateral responses. We further found that ON/OFF systems possess a larger response amplitude compared to ON/ON systems, due to the temporal structure and timing of the feedback. Our analysis supports the observation of oscillations in the electrosensory system when a sufficient number of neurons share common input. Our model was also used to reproduce

the response pattern found in the cat and guinea pig retina, where frequency doubling has been reported.

Even though the inclusion of OFF cells corresponds to a step toward more realistic models of early sensory systems, many physiological processes and components are believed to play an active part in information processing tasks of early sensory systems. Neural adaptation has been shown to influence the genesis of synchrony in recurrent networks [35, 36] as well as the formation of spatially organized activity patterns [37–40]. We thus expect that the timing and strength of adaptation might augment the range of response possibilities of ON/OFF nets and thus increase the physiological relevance of our model. The analysis of this problem is planned for later studies.

Inclusion of receptive field effects for both cell types is another obvious next step. This is also the case for the inclusion of other types of ON/OFF asymmetries seen, e.g., in retina where both onset and offsets of the stimulus can lead to increases of firing rates [41]. The connectivity between primary receptors and the ON and OFF cells considered here is known to determine receptive field properties and needs to be included in the analysis at some point. And finally, it will be interesting to determine whether the results found here in the context of asymmetric networks, where the ON and OFF cells can have different baseline or spontaneous activity, will respond to spatiotemporal stochastic signals in a way predicted by our analysis of deterministic signals here. This will reveal whether oscillations seen in data with spatially correlated stochastic stimuli are generically observed in ON/OFF cells, supporting our understanding of oscillations in the electrosensory system [11, 33, 34] and others with this type of forcing.

The circuitry investigated here assumes that both ON and OFF cells project to the same nucleus, which in turn feeds back symmetrically to all cells. The actual circuitry is not known in the electrosensory system, nor is it in most other systems. It may be that E cells project preferentially to E cells via the nucleus nP and I cells to I cells. Future work will investigate whether it is possible to make predictions of the true connectivity by using a clever suite of measurements. Of course, at the extreme where E's connect only to E's and I's only to I's, one is faced with two separate recurrent systems, both of which will obey the rules described here for ON/ON systems. Future work will also explore possible ways of performing a combination of closed loop experiments in order to reveal the spontaneous firing rates, thus enabling an estimate of V_o without tampering with the feedback.

References

1. Crook, S.M., et al.: The role of axonal delay in the synchronization of networks of coupled cortical oscillators. *J. Comput. Neurosci.* **4**, 161–172 (1997)
2. Ermentrout, G.B., Kopell, N.: Fine structure of neural spiking and synchronization in the presence of conduction delays. *Proc. Natl. Acad. Sci. U. S. A.* **95**, 1259–1264 (1998)
3. Roxin, A., et al.: The role of delays in shaping spatio-temporal dynamics of neuronal activity in large networks. *Phys. Rev. Lett.* **94**, 238103 (2005)
4. Campbell, S.A., et al.: Limit cycles, tori and complex dynamics in a second-order differential equation with delayed negative feedback. *J. Dyn. Diff. Equ.* **7**, 213 (1995)
5. Dhamala, M., Jirsa, V.K., Ding, M.: Enhancement of neural synchrony by time delay. *Phys. Rev. Lett.* **82**, 074104 (2004)
6. Masuda, N., Kazuyuki, A.: Bridging rate coding and temporal spike coding by effect of noise. *Phys. Rev. Lett.* **88**, 248101 (2002)
7. Borgeers, C., Kopell, N.: Synchronization in networks of excitatory and inhibitory neurons with sparse, random connectivity. *Neural Comput.* **15**, 509–538 (2003)
8. Foss, J., et al.: Multistability and delayed recurrent loops. *Phys. Rev. Lett.* **76**, 708–711 (1996)

9. Borgers, C., et al.: Gamma oscillations mediate stimulus competition and attentional selection in a cortical network model. *Proc. Nat. Acad. Sci. U. S. A.* **105**, 18023 (2008)
10. Marinazzo, D., et al.: Input-driven oscillations in networks with excitatory and inhibitory neurons with dynamic synapses. *Neural Comput.* **19**, 1739–1765 (2007)
11. Doiron, B., et al.: Oscillatory activity in electrosensory neurons increases with the spatial correlation of the stochastic input stimulus. *Phys. Rev. Lett.* **93**, 4 (2004)
12. Laing, C., Coombes, S.: The importance of different timings of excitatory and inhibitory pathways in neural field models. *Network* **17**, 151 (2006)
13. Blomquist, P., et al.: Localized activity patterns in two-population neuronal networks. *Physica D* **206**, 180 (2005)
14. Kandel, E.R., Schwartz, J.H.: *Principles of Neural Science*. Elsevier, New York (1983)
15. Robin, D.A., Royer, F.L.: Auditory temporal processing: two-tone flutter fusion and a model of temporal integration. *J. Acoust. Soc. Am.* **82**, 1207 (1987)
16. Fields, H.L., et al.: Dorsal horn projection targets of on and off cells in the rostral ventromedial medulla. *J. Neurophysiol.* **74**, 1742–1759 (1995)
17. Gollisch, T., Meister, M.: Modeling convergent on and off pathways in the early visual system. *Biol. Cybern.* **99**, 263–278 (2008)
18. Mehaffey, W.H., et al.: Intrinsic frequency tuning in ell pyramidal cells varies across electrosensory maps. *J. Neurophysiol.* **99**, 2641–2655 (2008)
19. Amthor, F.R., et al.: Morphologies of rabbit retinal ganglion cells with concentric receptive fields a–b. *J. Comp. Neurol.* **280**, 72–121 (1989)
20. Lefebvre, J., Longtin, A., LeBlanc, V.G.: Dynamics of driven recurrent networks of on and off cells. *Phys. Rev. E* **80**, 041912 (2009)
21. Hennig, M.H., et al.: The influence of different retinal subcircuits on the nonlinearity of ganglion cell behavior. *J. Neurosci.* **22**(19), 8726–8738 (2002)
22. Demb, J.B., et al.: Functional circuitry of the retinal ganglion cell’s nonlinear receptive field. *J. Neurosci.* **19**, 9756–9767 (1999)
23. Berman, N.J., Maler, L.: Neural architecture of the electrosensory lateral line lobe: adaptations for coincidence detection, a sensory searchlight and frequency-dependent adaptive filtering. *J. Exp. Biol.* **202**, 1243 (1999)
24. Pinto, D., Ermentrout, B.: Spatially structured activity in synaptically coupled neuronal networks: I–II. *SIAM J. Appl. Math.* **62**, 206–243 (2001)
25. Bressloff, P., et al.: Oscillatory waves in inhomogeneous neural media. *Phys. Rev. Lett.* **91**, 178101 (2003)
26. Jirsa, V.K.: Connectivity and dynamics of neural information processing. *Neuroinformatics* **2**, 183–204 (2004)
27. Coombes, S.: Waves, bumps, and patterns in neural field theories. *Biol. Cybern.* **93**, 91–108 (2005)
28. Lefebvre, J., Longtin, A., Leblanc, V.G.: Oscillatory response in a sensory network of ON and OFF cells with instantaneous and delayed recurrent connections. *Philos. Trans. R. Soc. Lond. Ser. A, Math. Phys. Eng. Sci.* **368**, 455–467 (2010)
29. Scholl, B., et al.: Nonoverlapping sets of synapses drive on responses and off responses in auditory cortex. *Neuron* **65**, 412–421 (2010)
30. Erneux, T.: *Applied Delay Differential Equations. Surveys and Tutorials in the Applied Mathematical Sciences*. Springer, New York (2009)
31. Folias, S.E., Bressloff, P.: Stimulus-locked waves and breathers in an excitatory neural network. *SIAM J. Appl. Math.* **65**, 2067 (2005)
32. Masuda, N., et al.: Coding of temporally varying signals in networks of spiking neurons with global delayed feedback. *Neural Comput.* **10**, 2139–2175 (2005)
33. Doiron, B., et al. Inhibitory feedback required for network oscillatory response to communication but not prey stimuli. *Nature* **421**, 539 (2003)
34. Lindner, B., et al.: Theory of oscillatory firing induced by spatially correlated noise and delayed inhibitory feedback. *Phys. Rev. E* **72**, 061919 (2005)
35. Ermentrout, B., et al.: The effects of spike frequency adaptation and negative feedback on the synchronization of neural oscillators. *Neural Comput.* **13**, 1285–1310 (2001)
36. Benda, J., et al.: Spike-frequency adaptation separates transient communication signals from background oscillations. *J. Neurosci.* **25**, 2312–2321 (2005)
37. Kilpatrick, Z.P., Bressloff, P.: Effects of synaptic depression and adaptation on spatiotemporal dynamics of an excitatory neuronal network. *Physica D* **239**, 547–560 (2009)
38. Coombes, S., et al.: Waves and bumps in neuronal networks with axo-dendritic synaptic interactions. *Physica D* **78**, 219–241 (2003)

39. Coombes, S., Owen, M.R.: Bumps, breathers, and waves in a neural network with spike frequency adaptation. *Phys. Rev. Lett.* **94**, 148102 (2005)
40. Folias, S.E., Bressloff, P.: Breathers in two-dimensional neural media. *Phys. Rev. Lett.* **95**, 208107 (2005)
41. Gao, J., et al.: An oscillatory circuit underlying the detection of disruptions in temporally-periodic patterns. *Network* **20**, 106–135 (2009)